Journal of Sound and Vibration 325 (2009) 884–893

Contents lists available at ScienceDirect

Journal of Sound and Vibration

journal homepage: www.elsevier.com/locate/jsvi

Low-frequency behavior in a frictionally excited beam

J.L. Quinby [1], B.F. Feeny *

Department of Mechanical Engineering, Michigan State University, 2555 Engineering Building, East Lansing, MI 48824, USA

ARTICLE INFO

Article history:
Received 4 April 2007
Received in revised form
29 March 2009
Accepted 30 March 2009
Handling Editor: C.L. Morfey
Available online 27 May 2009

ABSTRACT

A cantilevered beam excited by a periodically reciprocating friction contact surface exhibited extremely low-frequency responses (with frequencies as low as 100 times lower than the driver). Example responses near 1:1 and 1:2 resonances, between the excitation and the degree of freedom normal to the direction of sliding, show two-frequency quasiperiodicity, and in one case three-frequency quasiperiodicity. Underlying circle maps were extracted, and winding numbers were matched to response frequencies quantified in the fast Fourier transforms of the responses. A torus doubling bifurcation was documented.

1. Introduction

This paper documents extremely low-frequency responses of a beam, to a harmonically reciprocating contact surface, that had been casually observed in Ref. [1]. The mechanism of the low-frequency response in this experiment differs from that classified as subharmonic resonance [2], ultra-subharmonic responses [2–4], high-to-low-frequency modal energy transfer [5–11], frequency demultiplication [12], dither [13–17], and beating [18].

In this case, the dynamics are quasiperiodic with a strong very low-frequency. Quasiperiodicity itself is not unusual, and has been widely observed [19], both in forced systems (including those with or without a limit cycle, such as the van der Pol oscillator [2], the forced Rayleigh–Bénard experiment [20], and forced structures [21–23]), and autonomous systems (e.g. Bénard convection [24], and flow through a tube [25]), and many other systems. In the present case, the very low frequency may be an instance of slow effects of high-frequency excitation, examples of which include vibration feeders, autofocusing lenses, conveying fluid in vibrating pipes, and loosening bolts on vibrating machinery (see Ref. [26] and references within). The behavior observed here also supplements the possibilities for dynamic systems with friction, reviewed in Refs. [27,28].

The following includes a description of the experiment and examples of the low-frequency behavior.

2. Description of the experiment

The research presented here uses the same experimental setup as Ref. [1], wherein details can be found. Fig. 1 shows a general diagram of the experimental setup and Fig. 2 shows a transverse view of the two sections. The main beam (mild steel, $400 \times 12.8 \times 0.86\,\text{mm}^3$, $E = 128 \times 10^9\,\text{N/m}^2$, and density $\rho = 7488\,\text{kg/m}^3$) was clamped in the B-B section. The shaker is shown in the A-A section. The rectangle in the A-A section represents a steel block, attached to the shaker, oscillating out of the page in Fig. 1, providing a reciprocating friction contact. In the coordinate system *XYZ*, *X* is along the length of the main cantilever beam, *Y* is the flexural direction of the beam and *Z* is along the wide axis of the beam. The primary

* Corresponding author. Tel.: +1 517 353 9451; fax: +1 517 353 1750.
E-mail addresses: quinbyje@yahoo.com (J.L. Quinby), feeny@egr.msu.edu (B.F. Feeny).
[1] Tel.: +1 517 353 2980; fax: +1 517 353 1750.

0022-460X/$ - see front matter © 2009 Elsevier Ltd. All rights reserved.
doi:10.1016/j.jsv.2009.03.041

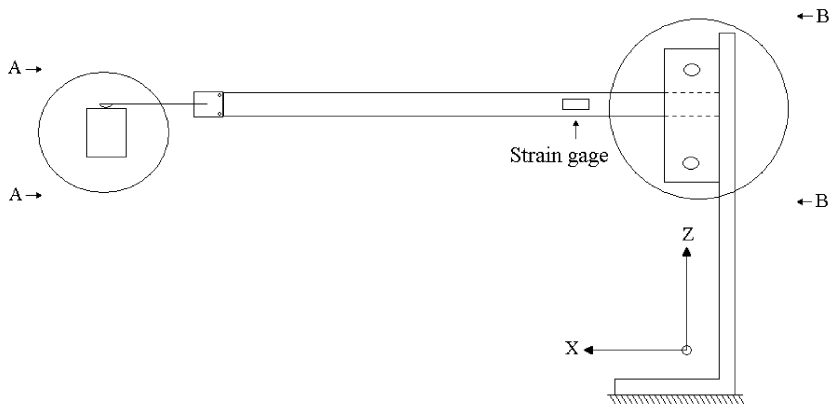

Fig. 1. Diagram of experimental setup.

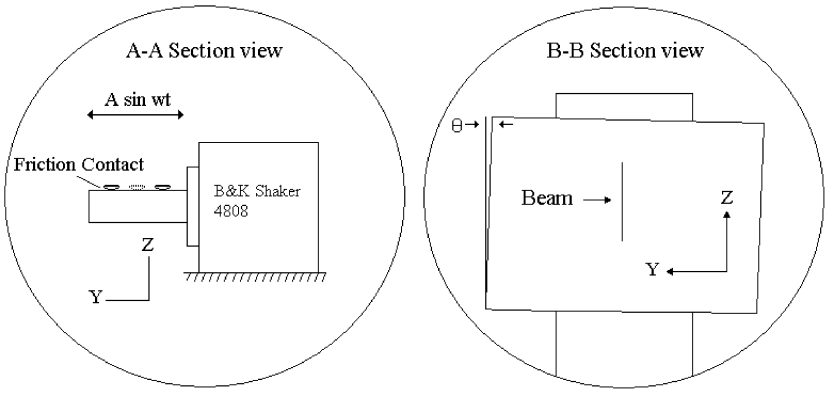

Fig. 2. Rotated view of sections A-A and B-B.

transverse beam deflection oscillation is in the Y direction. Attached to the end of the main beam, and penetrating the A-A circle in Fig. 1, is the "loading beam," which is flexible in the Z direction. The connecting fixture has a mass of 0.0123 kg. The end of the steel loading beam ($64 \times 13.4 \times 0.56\,\text{mm}^3$, $E = 126 \times 10^9\,\text{N/m}^2$, and density $\rho = 7488\,\text{kg/m}^3$) was in contact with the oscillating surface through a rubber tip, providing frictional excitation in the Y direction. The total length from clamp to tip is 464 mm. The previously measured force–velocity behavior [1] implied a tangentially compliant contact with a contact stiffness of $K_y = -20\,\text{kN/m}$ and a coefficient of sliding friction of $\mu = 0.55$.

The fixed end at B-B of the cantilever was slightly rotated in the Y–Z plane, such that the direction of flexure was slightly skewed with respect to the reciprocating steel surface, dominantly in the Y direction. This skewed alignment caused the normal load in A-A to vary with displacement, at a rate of about 0.035 N/cm. The load at the midpoint of the surface was 0.63 N. Over a 7 cm span of motion on the surface, the load ranged from 0.466 to 0.655 N. The varying normal force at the friction contact caused a varying friction force.

The cantilever beam deflection was sensed by a strain gage bending pair close to the clamped end. We sampled the signal $x(t)$ from the strain gage pair as an observer (in contrast to using several strain gage pairs for modal studies [1]) for phase-space reconstructions. Excitation and strain data were sampled at a rate of 5000 Hz, and the strain data were then linearly interpolated between up-crossings of the sinusoidal excitation through zero, thereby giving strain data that is sampled at each driving period, or in the Poincaré section. The notation $x(n)$ is used to indicate strain samples in the Poincaré section.

The Poincaré section was very useful because the beam tip moved very slowly, with a small superposed higher mode oscillation at the forcing frequency. The strain gage at the base of the beam magnified the higher-mode bending signal, emphasizing the forcing-frequency fluctuation much more than that observed in the tip motion. In the Poincaré section, the forcing-frequency fluctuation is omitted, thereby aiding visualization of the low-frequency dynamics.

2.1. System characteristics

We examined the linear behavior of both the clamped-free and the clamped-pinned beam, to represent sticking and slipping motions. The first five modal frequencies for the free beam were 2.5, 19.5, 57.5, 112 and 180 Hz. Loading the tip with

a large normal force, such that sliding was not likely to occur, approximated the linear pinned beam case. The lowest frequencies of the loaded modes were 13.5, 43.5, 93.0 and 171.5 Hz. During sliding, variation in the normal load with deflection in Y could excite the main beam in its stiff (Z) direction. The first Z-direction modal frequency of the loaded beam was 47 Hz. During frequency sweeps, the DC component of the response varied considerably [29].

3. Low-frequency response

Low-frequency behavior was observed when the excitation frequency was at a 1:1 or 1:2 resonance of the normal degree of freedom (47 Hz). We first show results for excitation in the range of 1:1 resonance, and then for the 1:2 resonance.

3.1. Results at 1:1 resonance

Movie 1 (in the online publication) displays, in a true time scale, the motion of the entire beam under an excitation of 45.7 Hz. Movie 2 shows the motion of the tip of the beam from above. In the movies, the input surface motion, and the higher modal component of the beam, both seem to beat. In fact, they do not really beat; this is due to the sampling distortion arising from the proximity of the 60 Hz video frequency and the 45.7 Hz driving frequency. The side view in Movie 3 reveals the motion of the normal degree of freedom. This motion does beat; it is active on the forward phase (into the image) of the tip, and ceases on the return phase. There is an audible, but not visible, tip chatter in the forward phase.

Fig. 3 shows the sequence of strains sampled in the Poincaré section for excitations of 45.2 and 45.6 Hz. The plotted samples are line-connected, as the responses are slow compared to the Poincaré-section sampling rate. The Poincaré section effectively strobed the strain signal at a fixed phase of excitation. The strobe removed the component of beam oscillation at the forcing frequency from the plot. The strobed tip motion of the beam was qualitatively similar to the strobed oscillation in Fig. 3, and spanned 2–5 cm peak to peak in this frequency range. The continuous time tip motion had an additional oscillation on the order of 1 mm in amplitude, at the driving frequency. The DC drift is a nonlinear (quadratic) effect.

Fig. 4 shows delay maps of the strain in the Poincaré section at 45.2 and 45.6 Hz, with delays of 5 and 3 samples. The former shows the cross-section of a torus whose corrugated and fuzzy portions might indicate torus wrinkling. The latter shows a doubled torus with mild corrugation.

Torus angles were defined in delay spaces with delays of 15 and 8 Poincaré-section samples for 45.2 and 45.6 Hz cases, whence the torus angle return plots were constructed (Fig. 5). Winding numbers of 0.00982 cyc/cyc at 45.2 Hz, and 0.0139 cyc/cyc at 45.6 Hz, were computed. The low winding numbers indicate that the iterates in Fig. 4 creep slowly around the closed loop, as opposed to dancing around the closed loops and filling in spaces. Reciprocals suggest that the torus windings were approximately 102 and 72 times slower than the driver, implying the "order" of the low-frequency component of each response (and giving a sense for the number of Poincaré-section samples per oscillation in Fig. 3). The circle maps for 45.2 and 45.6 Hz lie close to the diagonal, corresponding to the slow winding (small winding numbers). Since intermittency occurs with near tangencies of the circle map to the diagonal, the dynamics might be called "entirely intermittent" (an oxymoron). Overall, the dynamics are dominantly quasi-periodic. The doubled torus at 45.6 Hz is evident in the doubled circle map. A single-valued circle map could be obtained by redefining the angle modulus to cover two loops (4π radians) around the torus.

A 50 s segment of the strain measurement when the system was excited at 45.2 Hz was windowed with a Hanning window and a discrete (fast) Fourier transform of the result was taken to yield X_k. The magnitude, plotted in decibels, is shown in Fig. 6(a). A similar transformation of a 10,000 period segment of Hanning-windowed strain-gage data, $x(n)$, the

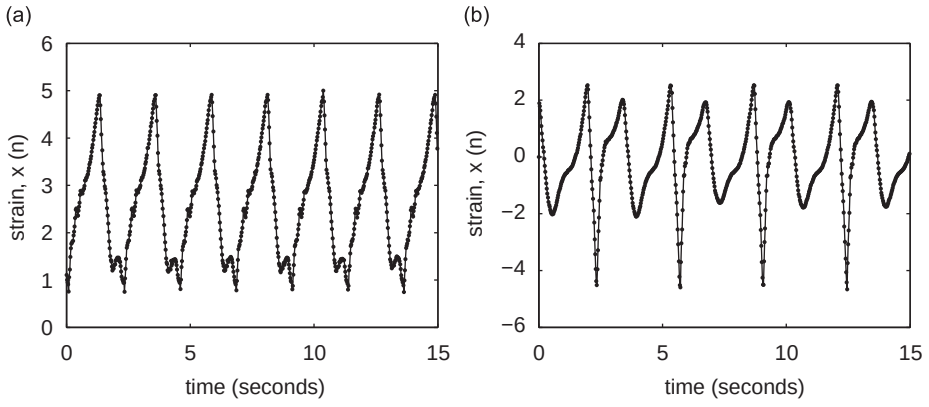

Fig. 3. Time histories of strain signals $x(n)$ sampled in the Poincaré section, at excitations of (a) 45.2 Hz, and (b) 45.6 Hz.

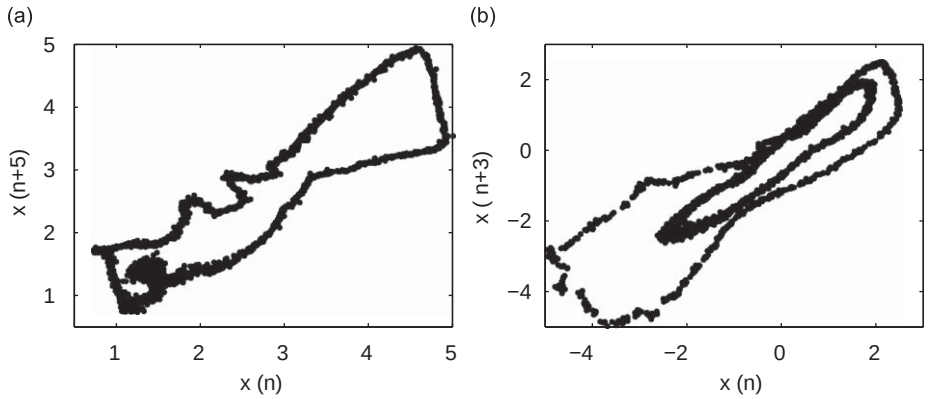

Fig. 4. Return maps on strain signals $x(n)$ in the Poincaré section for (a) 45.2 Hz excitation and a delay of 5 Poincaré-section samples, and (b) 45.6 Hz excitation and a delay of 3 Poincaré-section samples.

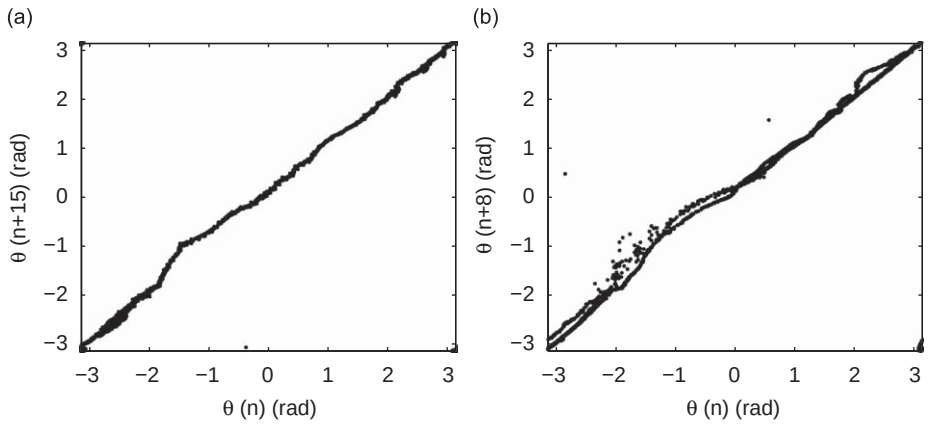

Fig. 5. Poincaré section torus angle return maps for (a) 45.2 Hz excitation, and (b) 45.6 Hz excitation.

Poincaré section, produced X_n^P, and the magnitude in decibels is plotted in Fig. 6(b). Similar spectra resulting from an excitation at 45.6 Hz are shown in Fig. 7. The spectrum in the Poincaré section magnifies the resolution at low frequencies, and removes the driving frequency.

The spectrum of the 45.2 Hz case shows the lowest spike at 0.44 Hz. The behavior includes interactions of two dominant frequencies with the "subharmonic" occurring on the order of about 103, in agreement with the order obtained from the winding number. Here, the word "subharmonic" refers to a strong component of the response at a frequency lower than the driving frequency, and the word "order" represents the ratio of the driving frequency to the "subharmonic" frequency. The 45.2 Hz driver and 0.44 Hz component suggest two-frequency quasi-periodicity. While the strain signal showed two dominant frequencies, in the tip displacement the low frequency was strongest, similar to the response shown in the movies. Technically, the "subharmonic" may not be a harmonic, rather an "undertone", as the driving frequency and the "subharmonic" frequency are not commensurate.

The spectrum of 45.6 Hz case, displayed in Fig. 7, has a similar behavior to the 45.2 Hz case, except the second "subharmonic" is dominant. The winding number of 0.0139 cyc/cyc, when multiplied by 45.6 Hz, confirms the "subharmonic" frequency of 0.6 Hz and is associated with the main (undoubled) torus, at a "subharmonic order" of approximately 76. The 0.3 Hz is then a subharmonic resonance of the 0.6 Hz component, associated with torus doubling. This subharmonic is at an order of 152 with respect to the excitation! The dynamics are classified as two-frequency quasi-periodic with torus doubling.

The torus doubling bifurcation (e.g. [19,30–33]) is witnessed in Fig. 8. Starting at 46 Hz we swept down slowly to 45.84 Hz, where the torus-doubling phenomenon began. There are two cases at 45.84 Hz. In the first one case there is no indication of a torus doubling, while a little while later data was taken at that same frequency and the torus doubling had become active. As the frequency was increased again, the doubled torus disappeared. (These data were obtained several days after that of Figs. 3–5, with slightly different ambient conditions, and so the driving frequencies are not exactly the same.) Other systems have shown finite torus doublings to chaos [34] and torus-doubling cascades to chaos (e.g. [21–23,35,36], or see Ref. [19]).

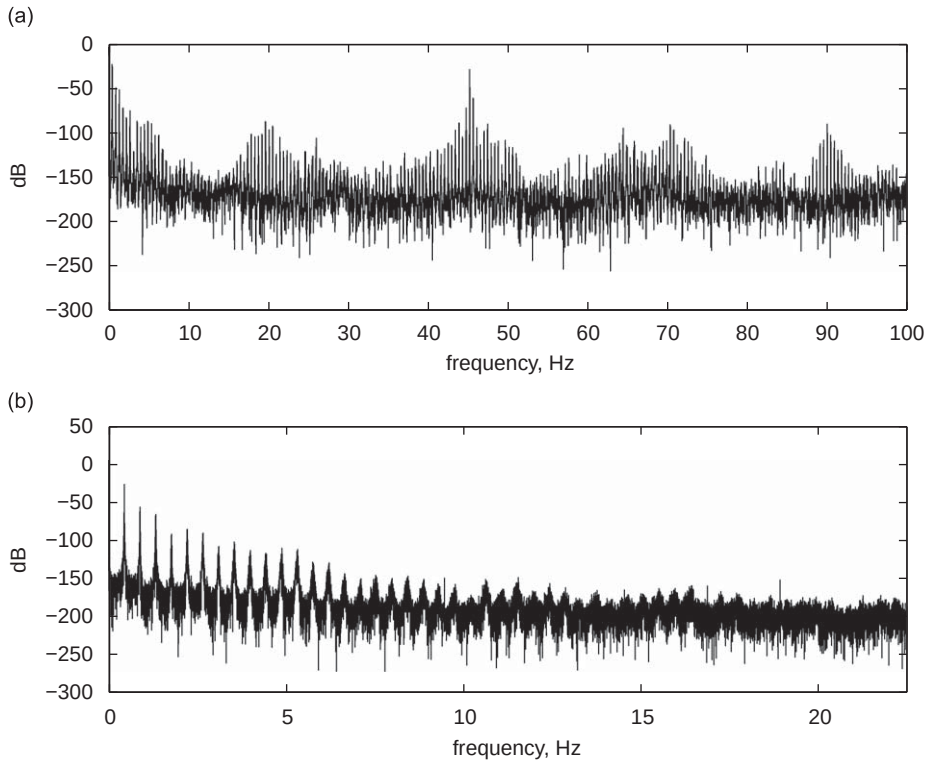

Fig. 6. Fourier spectra of the signals from (a) 50 s of strain data, $x(t)$, sampled at 200 Hz, after using a Hanning window, and (b) 10,000 periods (221 s) of Poincaré-section data, $x(n)$, after using a Hanning window, for the excitation at 45.2 Hz. In the figures, dB refers to (a) $20\log_{10}|X_k|$, and (b) $20\log_{10}|X_n{}^P|$.

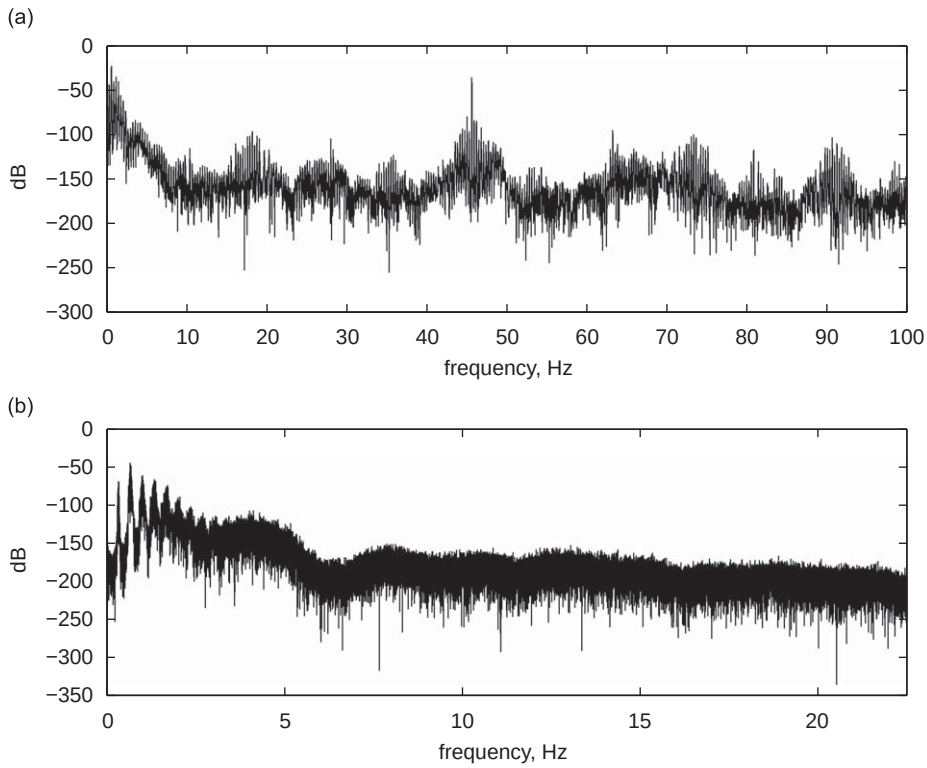

Fig. 7. Spectra of the signals from (a) 50 s of strain data, $x(t)$, sampled at 200 Hz, after using a Hanning window, and (b) 10,000 periods (219 s) of Poincaré-section data, $x(n)$, after using a Hanning window, for the excitation at 45.6 Hz. In the figures, dB refers to (a) $20\log_{10}|X_k|$, and (b) $20\log_{10}|X_n{}^P|$.

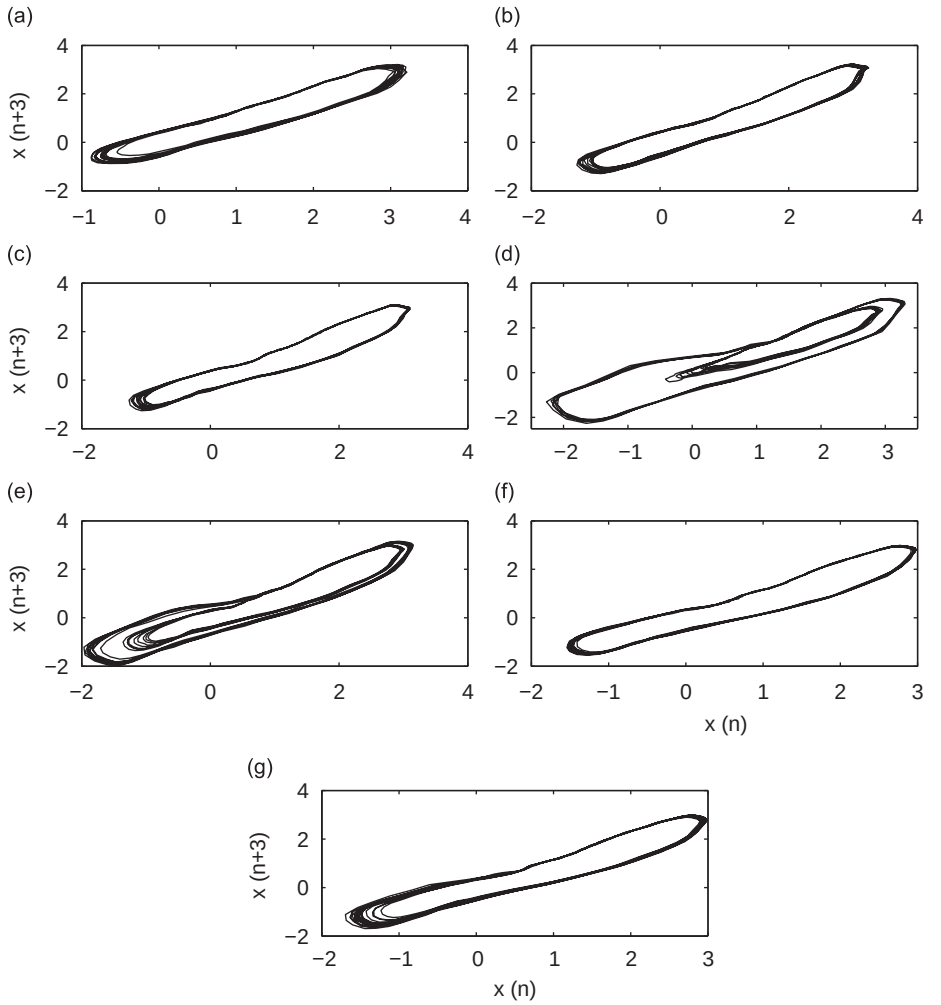

Fig. 8. Example of torus doubling with varying excitation frequency, in the Poincaré section delay space with a delay of three samples. The original torus destabilizes and doubles at a driving frequency of 45.84 Hz. In plots (a)–(c), the excitation frequency is very slowly decreased, and in plots (e)–(g) the excitation frequency is very slowly increased. The excitation frequencies are (a) 46 Hz, (b) 45.88 Hz, (c) 45.84 Hz, (d) 45.84 Hz, (e) 45.85 Hz, (f) 45.857 Hz, and (g) 45.859 Hz.

During all of these responses (Figs. 1–8), the normal degree of freedom was visibly active, and was likely excited by the variation in the normal load due to the slight skewness in the surface/bending alignment, or possibly by microscale dynamics in the normal degree of freedom, the existence of which has been suggested by some friction experimenters and modelers [37–39]. The beam's normal vibration had beats that synchronized with the phase of the tip. The normal degree of freedom, at least one transverse mode, and the excitation provide at least five state-space dimensions, sufficient to allow torus doubling.

The excitation frequencies were near the frequency of the normal degree of freedom (44.7 Hz). The 0.44 Hz nearly matched the difference 45.2–44.7 Hz, and likewise, the 0.6 Hz is close to $\frac{2}{3}$ the difference. (The doubled torus frequency is $\frac{1}{3}$, but the "primary" torus would be the object of interest in these interactions.) In both cases, it is possible that a nonlinear combination of the excitation and the normal and transverse degrees of freedom organizes itself as a slow tip motion of the low-frequency difference. In both cases, the low frequency term is the dominant peak, even in the strain gage signals (i.e. more so in the beam tip signals, as mentioned, and as would be guessed from viewing the movies.)

The low frequencies of the beam tip motion matched the 0.44 and 0.6 Hz frequencies as seen in the Fourier spectra, which are well below (5.7 and 4.16 times), and likely incommensurate to, the first clamped-free modal frequency. To an observer, the creeping beam tip, well below its dynamic range, actually seemed devoid of inertial effects. Indeed, comparing $\ddot{x}$ and $\omega_n^2 x$ terms of a single-degree-of-freedom first-mode model, the amplitude of the inertial force for the low harmonic was 32 and 17 times smaller than the associated linearized stiffness force in the oscillator, suggesting nearly quasi-static motion. This contrasts the typical case in which the inertia is an essential component of a mechanical oscillator.

Quasiperiodicity itself is not unique. The quasiperiodicity here was likely due to nonlinear coupling between the excitation, modal, and normal-degree-of-freedom frequencies. It is possible that quasi-static or kinematic relationships play a role here. It is curious that the lower-frequency component was significantly below the natural and applied frequencies of the forced vibration system, yet was not primarily a beating effect, in the sense that the tip motion did not consist of a slowly varying amplitude of higher frequency oscillation, typical of beating.

3.2. Results near 1:2 resonance

Very low-frequency responses were also observed at excitation frequencies in the range of about half of the normal-degree-of-freedom natural frequency (also about half of the second modal frequency of the "pinned" beam), and results are shown for a driving frequency of 21.9 Hz. Fig. 9(a) shows the strain sampled in the Poincaré section and plotted against the sample time. The dynamics show a phase of considerable oscillation, and then a phase of slow motion, in the Poincaré section. The strain in the Poincaré section is plotted against its next delay in Fig. 9(b). The dark band in the delay plot corresponds to the slower phase of motion, while the cloud of points corresponds to the oscillation seen in the Poincaré-sectioned response. As in the 1:1 case above, the Poincaré sectioning conceals the contribution, to the strain signal, of a

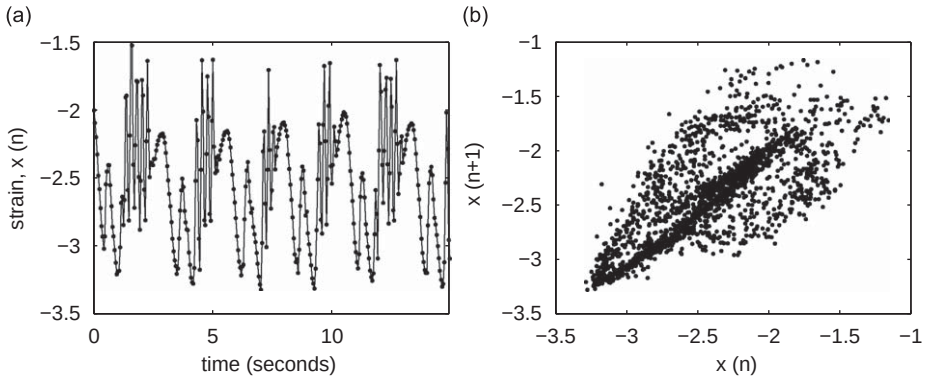

Fig. 9. (a) Time histories of strain signals $x(n)$ sampled in the Poincaré section, at an excitation of 21.9 Hz. (b) Return map on strains $x(n)$ in the Poincaré-section for 21.9 Hz excitation with a delay of 1 Poincaré-section sample.

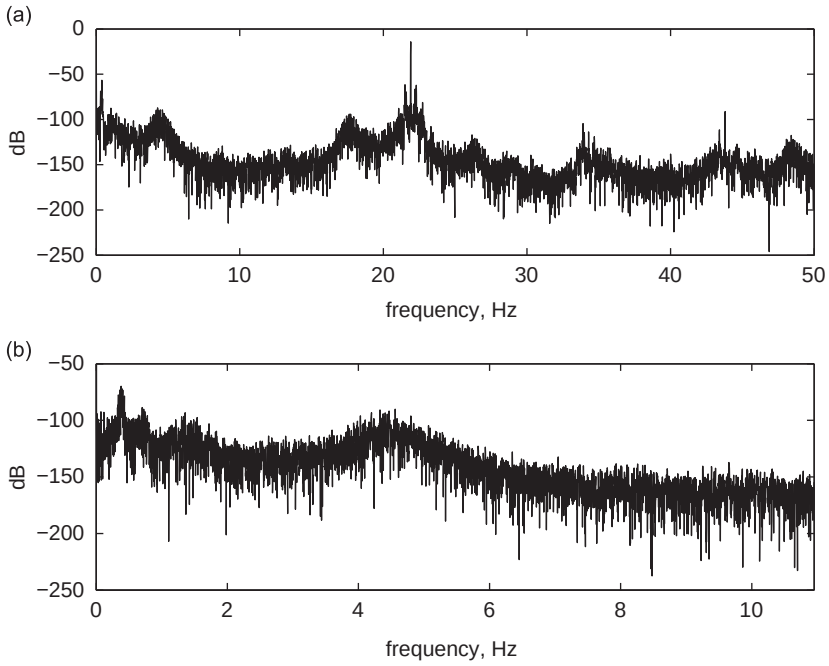

Fig. 10. Spectra of the signals from (a) 100 s of strain data $x(t)$, sampled at 100 Hz, after Hanning windowing, and (b) 10,000 periods (457 s) of Poincaré-section data $x(n)$ after windowing, for the excitation at 21.9 Hz. In the figures, dB refers to (a) $20\log_{10}|X_k|$, and (b) $20\log_{10}|X_n{}^P|$.

superposed forced beam vibration at the driving frequency of 21.9 Hz, and is more representative of the wandering beam tip.

The spectrum of the Hanning-windowed sampled strain $x(t)$ is shown in Fig. 10(a). There is a dominant peak at 21.9 Hz corresponding to the oscillatory strain of superposed forced beam vibration at the driving frequency. The spectrum also indicates a peak at about 0.4 Hz, which corresponds to the main frequency of the wandering tip. This 0.4 Hz is also the frequency difference between the driving frequency and the frequencies of the small peaks right next to it. There is a suppressed peak at 4.3 Hz, which also marks the difference between the 21.9 Hz peak and the subtle humps on either side. The spectrum of the strain signal $x(n)$ in the Poincaré-section is shown in Fig. 10(b), which again removes the driving frequency information and emphasizes the low-frequency content. The presence of three seemingly independent frequencies suggests three-frequency quasiperiodicity, or narrowband chaos with the slightly raised spectrum near the peaks. The ratio of the driving frequency and the low frequency peak suggests a "subharmonic order" of about 55. Since the Poincaré section delay map produced a cloud of data, rather than a closed curve of data, we were unable to construct an underlying circle map with an estimated winding number.

Fig. 11 shows the time history and delay map of the strain signal in the Poincaré section for responses to a 22.3 Hz driving frequency. In the delay map of Fig. 11(b), iterated points proceed clockwise around the light cloud, and then get trapped on the much slower dark band, before resuming travel on the light cloud. A circle map was recovered in this case (Fig. 12). The dark band of Fig. 11(b) coincides with that part of the circle map that is tangential to the diagonal. This might either be indicative of dynamics that are more complicated than a true one-dimensional circle map (for example with wrinkling), or a feature that is caused by the projection, of the iterates on a closed curve, to the two-dimensional plot. Nonetheless, from the circle map construct, the winding number was estimated to be 0.0306 cyc/cyc. The spectrum (not shown) indicates peaks at the driving frequency and at 0.68 Hz, suggesting a "subharmonic order" of 32.8, which is

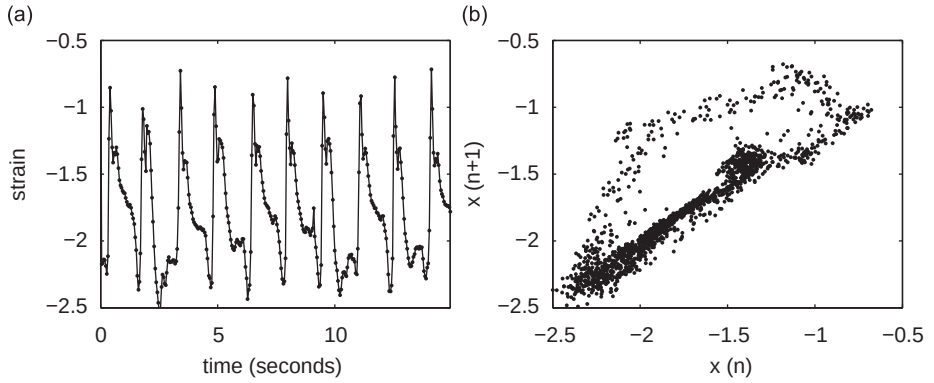

Fig. 11. (a) Time histories of strain signals $x(n)$ sampled in the Poincaré section, at an excitation of 22.3 Hz. (b) Return map on strains $x(n)$ in the Poincaré-section for 22.3 Hz excitation with a delay of 1 Poincaré-section sample.

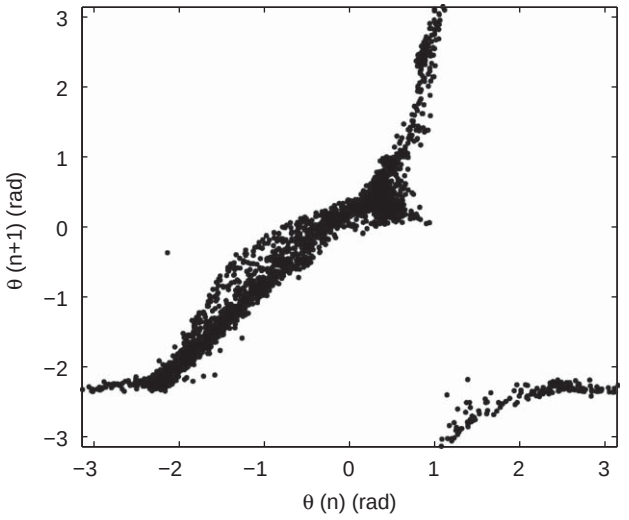

Fig. 12. Poincaré section torus angle return map for the case of 22.3 Hz excitation.

consistent with the winding number reciprocal (32.7). The alternation between the quicker cloud of points and the slow, dark band, is similar to the features of the 21.9 Hz case. However, in this case, the spectra suggest the dynamics were born from two-frequency quasiperiodicity.

The above examples occurred at excitation frequencies slightly below one half of the normal degree of freedom frequency. Although not shown (see Refs. [29,40]), we have also observed two-frequency toroidal dynamics at frequencies slightly higher than one half of this frequency. In these cases, circle maps indicated intermittency. Fourier spectra and circle maps showed "subharmonic orders" of the range of about 11–12.

3.3. Comments

A mechanism for generating at least some of the very low-frequency responses is conjectured. The normal degree of freedom is resonated such that it cyclically increases and decreases the contact load. With sufficiently increased contact load, a short-time stick allows the tip to creep on the reciprocating surface. The quasi-statically creeping tip either slips on the return, or reverses itself with the varying phase between the surface and the normal degree of freedom, consistent with the match in the low-frequency tip and the difference between the driver and the normal degree of freedom suggested in the first example. Our next step will be to explain the behavior with the derivation of a low-order model, and its analysis, perhaps using perspective of Thomsen and colleagues [16,26], geared for describing the slow effects of fast excitations and later used for dither [17]. In this perspective, the response is expanded as a slow component plus a fast oscillation (in contrast to the usual fast oscillation with a slowly varying amplitude).

4. Conclusions

A cantilevered beam excited by a periodically reciprocating friction contact exhibited very low-frequency responses, much below the fundamental frequency of the system. These very low-frequency responses often were seen to involve beam oscillations normal to the contact surface, at the frequency of the normal degree of freedom. We documented example responses near 1:1 and 1:2 resonances with this normal degree of freedom. For the observed 1:1 resonance case, from the underlying circle maps and spectra, the dynamics is two-frequency quasiperiodic with imminent torus wrinkling. An example of torus doubling was also exhibited. For the 1:2 resonance range, it is concluded from examination of the spectra that dynamic responses could involve two or three incommensurate frequencies.

The low-frequency behavior here is a different phenomenon from true subharmonic resonance, frequency demultiplication, and the high-to-low modal energy transfer. Although the normal degree of freedom exhibits beats (synchronized with the tip motion), the slowly moving beam tip did not beat. The unusual aspect of the response was that it occurs at frequencies well below those of the dynamics of the system. It may fit best with the phenomena suggested in [26]. This work presented the observation of a phenomenon without an analysis on how the behavior arose, and so an explanation with modeling and analysis would be the next step.

Acknowledgements

This work is based upon research supported by the National Science Foundation under Grant no. CMS-0099603. Any opinions, findings, and conclusions or recommendations expressed in this material are those of the author and do not necessarily reflect the views of the National Science Foundation. We thank Professors Dean Mook, Richard Rand, Steve Shaw, and Alan Haddow for their comments.

Appendix A. Supplementary material

Supplementary data associated with this article can be found in the online version at doi:10.1016/j.jsv.2009.03.041.

References

[1] R.V. Kappagantu, B.F. Feeny, Part 1: dynamical characterization of a frictionally excited beam, *Nonlinear Dynamics* 22 (2000) 317–333.
[2] A.H. Nayfeh, D.T. Mook, *Nonlinear Oscillations*, Wiley, New York, 1979.
[3] M. Qriouet, C. Mira, Fractional harmonic synchronization in the Duffing–Rayleigh differential equation, *International Journal of Bifurcation and Chaos in Applied Sciences and Engineering* 4 (2) (1994) 411–426.
[4] K. Yagasaki, Higher-order averaging and ultra-subharmonics in forced oscillators, *Journal of Sound and Vibration* 210 (4) (1998) 529–553.
[5] A.G. Haddow, S.M. Hasan, Nonlinear oscillation of a flexible cantilever: experimental results, *Proceedings of the Non-Linear Vibrations, Stability, and Dynamics of Structures and Mechanisms Conference*, Blacksburg, VA June 1–3, 1988.
[6] S.A. Nayfeh, A.H. Nayfeh, Nonlinear interactions between two widely spaced modes—external excitation, *International Journal of Bifurcation and Chaos* 3 (2) (1993) 417–427.
[7] S.A. Nayfeh, A.H. Nayfeh, Energy-transfer from high-frequency to low-frequency modes in a flexible structure via modulation, *Journal of Vibration and Acoustics* 116 (2) (1994) 203–207.

[8] A.H. Nayfeh, D.T. Mook, Energy-transfer from high-frequency to low-frequency modes in structures, *Journal of Mechanical Design* 117 (1995) 186–195 (Special issue B).
[9] A.H. Nayfeh, C.-M. Chin, Nonlinear interaction in a parametrically excited system with widely spaced frequencies, *Nonlinear Dynamics* 7 (1995) 195–216.
[10] K. Oh, A.H. Nayfeh, High- to low-frequency modal interactions in a cantilever composite plate, *Journal of Vibration and Acoustics* 120 (2) (1998) 579–587.
[11] T.J. Anderson, A.H. Nayfeh, B. Balachandran, Coupling between high-frequency modes and a low-frequency mode: theory and experiment, *Nonlinear Dynamics* 11 (1996) 17–36.
[12] Balth. Van Der Pol, J. Van Der Mark, Frequency demultiplication, *Nature* 120 (1927) 363–364.
[13] N.N. Minorsky, *Nonlinear Oscillations*, Van Nostrand, Princeton, NJ, 1962 (Chapter 24).
[14] J.J. Stoker, *Nonlinear Vibrations in Mechanical and Electrical Systems*, Interscience Publishers, New York, 1950.
[15] G. Zames, N.A. Schneydor, Dither in nonlinear systems, *IEEE Transactions on Automatic Control* 21 (1976) 660–667.
[16] J.J. Thomsen, Using fast vibrations to quench friction-induced oscillations, *Journal of Sound and Vibration* 228 (1999) 1079–1102.
[17] B.F. Feeny, F.C. Moon, Quenching stick-slip chaos with dither, *Journal of Sound and Vibration* 237 (1) (2000) 173–180.
[18] Z.L. Zhang, Q.T. Tao, Experimental study of non-linear vibrations in a loudspeaker cone, *Journal of Sound and Vibration* 248 (1) (2001) 1–8.
[19] A.H. Nayfeh, *Nonlinear Interactions. Analytical, Computational, and Experimental Methods*, Wiley, New York, 2000.
[20] M.H. Jensen, L.P. Kadanoff, A. Libchaber, I. Procaccia, J. Stavans, Global universality at the onset of chaos: results of a forced Rayleigh–Bénard experiment, *Physical Review Letters* 55 (25) (1985) 2798–2801.
[21] B. Balachandran, A.H. Nayfeh, Observations of modal interactions in resonantly forced beam-mass structures, *Nonlinear Dynamics* 2 (1999) 77–117.
[22] J.M. Johnson, A. Bajaj, Amplitude modulated and chaotic dynamics in resonant motion of strings, *Journal of Sound and Vibration* 128 (1) (1989) 87–107.
[23] T.L.A. Molteno, N.B. Tufillaro, Torus doubling and chaotic string vibrations—experimental results, *Journal of Sound and Vibration* 137 (2) (1990) 327–330.
[24] P. Berge, Y. Pomeau, C. Vidal, *Order Within Chaos, Towards a Deterministic Approach to Turbulence*, Wiley, New York, 1984.
[25] G.S. Copeland, F.C. Moon, Chaotic flow-induced vibration of a flexible tube with end mass, *Journal of Fluids and Structures* 6 (6) (1992) 705–718.
[26] D. Tcherniak, J.J. Thomsen, Slow effects of fast harmonic excitation for elastic structures, *Nonlinear Dynamics* 17 (3) (1998) 227–246.
[27] R.A. Ibrahim, Friction-induced vibration, chatter, squeal, and chaos: part I & II—mechanics of friction, *Friction-Induced Vibration, Chatter, Squeal and Chaos* DE-49 (1992) 107–138.
[28] B. Armstrong-Hélouvry, P. Dupont, C. Canudas de Wit, A survey of models, analysis tools and compensation methods for the control of machines with friction, *Automatica* 30 (7) (1994) 1083–1138.
[29] J.L. Quinby, Nonlinear Dynamics of a Frictionally Excited Cantilever Beam, M.S. Thesis, East Lansing, 2003.
[30] K. Kaneko, Doubling of torus, *Progress of Theoretical Physics* 69 (6) (1983) 1806–1810.
[31] V. Franceschini, Bifurcations of tori and phase locking in a dissipative system of differential equations, *Physica D* 6 (3) (1983) 285–304.
[32] A.C. Skeldon, T. Mullin, Mode interaction in a double pendulum, *Physics Letters A* 166 (3-4) (1992) 224–229.
[33] A. Cros, E. Floriani, P. Le Gal, R. Lima, Transition to turbulence of the Batchelor flow in a rotor/stator device, *European Journal of Mechanics B/Fluids* 24 (2005) 409–424.
[34] J.C. Shin, Experimental observation of a torus-doubling transition to chaos near the ferroelectric phase transition of a KH2PO4 crystal, *Physical Review E* 60 (5) (1999) 5394–5401.
[35] M. Sekikawa, T. Miyoshi, N. Inaba, Successive torus doubling, *IEEE Transactions on Circuits and Systems I—Fundamental Theory and Applications* 48 (1) (2001) 28–34.
[36] A. Arneodo, P.H. Coullet, E.A. Spiegel, Cascade of period doublings of tori, *Physics Letters A* 94 (1) (1983) 1–6.
[37] D.M. Tolstoi, Significance of the normal degree of freedom and the natural normal vibrations in contact friction, *Wear* 10 (1967) 199–213.
[38] J.T. Oden, J.A.C. Martins, Models and computational methods for dynamic friction phenomena, *Computer Methods in Applied Mechanics and Engineering* 52 (1–3) (1985) 527–634.
[39] H. Dankowicz, On the modeling of dynamic friction phenomena, *Zeitschrift fuer angewandte Mathematik und Mechanik* 79 (6) (1999) 399–409.
[40] J.L. Quinby, B.F. Feeny, Low-frequency phenomena in a frictionally excited beam, *Proceedings of the ASME International Design Engineering Technical Conferences*, Anaheim, November 13–19, 2004, paper number IDETC2004-59779 on CD-ROM.